Nitro-chloromethylbenzindolines: hypoxia-activated prodrugs of potent adenine *N*3 DNA minor groove alkylators

William R. Wilson, Stephen M. Stribbling, Frederik B. Pruijn, Sophie P. Syddall, Adam V. Patterson, H.D. Sarath Liyanage, Eileen Smith, K. Jane Botting, and Moana Tercel

Auckland Cancer Society Research Centre, Faculty of Medical and Health Science, The University of Auckland, Auckland, New Zealand

Abstract

Hypoxia represents an important therapeutic target in tumors because of the resistance of hypoxic cells to radiotherapy and chemotherapy and because it is more severe in many tumors than in normal tissues. Here, we describe a class of prodrugs, nitro-chloromethylindolines, which undergo hypoxia-selective activation by endogenous nitroreductases in tumor cells to form the corresponding amino compounds. The latter are chemically related to the cyclopropylindoline antitumor antibiotics and they share the same properties of sequence-selective DNA minor groove alkylation and high cytotoxic potency. Of three alkylating subunits investigated, the chloromethylbenzindoline (CBI) structure provided the most favorable prodrug properties: aerobic cytotoxic potency of the amines was approximately 90- to 3,000-fold higher than the corresponding nitro compounds, and the nitro compounds showed air/anoxia potency differentials of up to 300-fold. Selective alkylation of adenine *N*3 in calf thymus DNA by an amino-CBI was shown by characterization of the thermal depurination product; the same adduct was shown in hypoxic RIF-1 cells exposed to the corresponding nitro-CBI prodrug under hypoxic (but not oxic) conditions. The amino metabolite generated from a nitro-CBI by cells expressing *Escherichia coli nfsB* nitroreductase in multicellular layer cultures was shown to elicit bystander killing of surrounding cells. Nitro-CBI prodrugs were >500-fold less toxic to mice than amino-CBIs by i.p. administration and provided selective killing of hypoxic cells in RIF-1 tumors (although only at maximally tolerated doses). Nitro-CBIs are novel lead hypoxia-activated prodrugs that represent the first examples of hypoxia-selective generation of potent DNA minor groove alkylating agents. [Mol Cancer Ther 2009;8(10):2903–13]

Introduction

Severe hypoxia arises in tumors as a result of a structurally and functionally abnormal microvascular system and plays a major role in tumor progression (1). Hypoxia also represents an obstacle for all major forms of cancer therapy. For example, the higher frequency of metastasis from more severely hypoxic tumors potentially compromises outcomes of surgery (2) and radiotherapy (3). Hypoxia also confers resistance of the primary tumor to ionizing radiation (4) and compromises chemotherapy through multiple mechanisms (5). These include inaccessibility of hypoxic cells to blood-borne drugs, low proliferative activity in hypoxic regions of tumors, selection of cells with reduced sensitivity to apoptosis, and the induction of molecular responses to hypoxic stress that exacerbates drug resistance. These features make hypoxic tumor cells an important therapeutic target.

In addition, because hypoxia is more extensive and severe in tumors than in normal tissues (6), it represents a selective tumor target. These considerations have resulted in much interest in designing prodrugs that are activated selectively by metabolic reduction within hypoxic regions of tumors (5, 7, 8). These hypoxia-activated prodrugs (HAP) act as direct oxygen sensors through the ability of O_2 to inhibit the first step in their reductive metabolism, usually by reoxidizing the initial radical intermediate (9). Several HAPs are currently in clinical trial (*N*-oxides tirapazamine and banoxantrone, nitro compounds PR-104 and TH-302, and quinones apaziquone and RH1), and the approved drug mitomycin C has weak selectivity for hypoxic cells (10).

Preclinical and clinical evaluation of HAP has identified several critical requirements, which, arguably, are not present optimally in any of the above agents. In particular, some are substrates for competing activation by oxygen-independent two-electron reductases, as shown for apaziquone (10), RH-1 (11), and PR-104 (12), which limits their selectivity for hypoxia. Some penetrate poorly into hypoxic regions of tumors, as shown for tirapazamine (13) and

Received 4/17/09; revised 8/4/09; accepted 8/18/09; published OnlineFirst 10/6/09.

Grant support: Foundation for Research, Science and Technology, New Zealand, grants UOAX0211 and UOAX0703.

The costs of publication of this article were defrayed in part by the payment of page charges. This article must therefore be hereby marked *advertisement* in accordance with 18 U.S.C. Section 1734 solely to indicate this fact.

Note: Supplementary material for this article is available at Molecular Cancer Therapeutics Online (http://mct.aacrjournals.org/).

Current address for S.M. Stribbling: CRT Discovery Laboratories, The Cruciform Building, Gower Street, London WC1E 6BT, United Kingdom. Current address for E. Smith: Watercare Services Ltd., P. O. Box 107028, Airport Oaks, Manukau 2154, New Zealand.

Requests for reprints: William R. Wilson, Auckland Cancer Society Research Centre, Faculty of Medical and Health Science, The University of Auckland, Private Bag 92019, Auckland, New Zealand. Phone: 64-9-3737599, ext. 86886; Fax: 64-9-3737571. E-mail: wr.wilson@auckland.ac.nz

doi:10.1158/1535-7163.MCT-09-0571

apaziquone (14). In addition, tirapazamine is activated at relatively high oxygen concentrations (15), which may contribute to its toxicity in normal tissues (16, 17). Further, with the exception of PR-104 and related dinitrobenzamide mustards (18–20), there is little evidence for bystander effects resulting from diffusion of active (reduced) metabolites from hypoxic zones. This feature is likely to be important for successful exploitation of hypoxia by HAP because it removes the requirement for metabolic activation in every hypoxic cell and, in particular, allows killing of hypoxic cells at oxygen concentrations too high to activate HAPs but low enough to be resistant to conventional cytotoxics (18, 20). A further limitation with existing HAP is that the resulting active metabolites generally fall within chemical classes that are subject to multidrug resistance (e.g., nitrogen mustards and topoisomerase II poisons), which may limit their utility.

These considerations have led us to explore a novel class of HAP with the potential to address these limitations. The cyclopropylindoline antitumor antibiotics, exemplified by CC-1065 and duocarmycin SA, alkylate *N*3 of adenine in a sequence-selective manner in the minor groove of DNA and are some of the most potent cytotoxic agents known (21). Several analogues have shown antitumor activity in preclinical models (22), and four (adozelesin, carzelesin, bizelesin, and KW-2189) were evaluated clinically. All lacked antitumor activity at their maximum tolerated doses (MTD), which were limited by myelotoxicity to which humans seemed to be considerably more sensitive than mice (23). We have developed synthetic analogues of the cyclopropylindolines in which the key phenol of the alkylating subunit is replaced by an amino functional group (amino-chloromethylindolines; refs. 24–26). This structural change generates agents that share many of the same properties as the phenolic compounds (26–28) but allows the possibility that the corresponding nitro compounds might act as HAP through bioreduction via an initial oxygen-sensitive one-electron step to the amino-chloromethylindolines. We have shown that one particular example of a nitro-cyclopropylindoline [termed nitro-CI-5,6,7-trimethoxyindole (TMI) in the present study] becomes 400-fold more cytotoxic *in vitro* when activated by the *Escherichia coli nfsB* nitroreductase (NTR; ref. 29), but have not previously examined whether these compounds can be activated by mammalian enzymes under hypoxic conditions.

Here, we evaluate a series of nitro-cyclopropylindoline derivatives to identify candidates with potential as HAP and explore the mechanism of action and therapeutic utility of a preferred subclass (nitro-CBIs) in preclinical models.

Materials and Methods

Compounds

The amino and nitro compounds of Fig. 1A were synthesized as reported previously (25, 26, 30, 31). Stock solutions in DMSO were stored at −80°C. Chlorambucil was purchased from Sigma. Tirapazamine and the NTR substrates CB 1954 and SN 27686 (32) were synthesized in this laboratory. The adenine adduct of amino-CBI-TMI was prepared by reaction with calf thymus DNA followed by thermal depurination, essentially as described for amino-CI-TMI (27); details of adduct isolation and characterization are given in Supplementary Materials and Methods.

Cell Lines

Origins of the repair-competent Chinese hamster ovary cell line AA8 and its repair-defective mutants are given in Supplementary Table S1. Sources of the human tumor cell lines (HT29, SKOV3, HCT8, and HCT116) are as previously described (19). RIF-1 and EMT6 murine tumor lines were from Dr. J. Martin Brown (Stanford University). The origin of the HCT116-NTR^{puro} line, which stably expresses NTR, has been described (32). All cell lines were maintained in α-MEM containing 5% to 10% of fetal bovine serum without antibiotics and reestablished every 3 mo from frozen stocks confirmed to be free of *Mycoplasma* by PCR-ELISA (Roche Diagnostics).

Cytotoxicity Assays

Antiproliferative potency was determined using 4-h exposure of cells in 96-well plates under aerobic conditions at pH 7.4 as previously described (19) or at pH 6.5 by acidification acutely during drug exposure or chronically for 18 h before and during drug exposure. Details of adjustment of pH are given in Supplementary Materials and Methods. Clonogenic assays for cell sterilization under aerobic and hypoxic conditions were done using stirred and continuously gassed (5% CO_2 in air or N_2, respectively) cell suspensions (10^6 cells/mL) as previously described (20). The hypoxic cytotoxicity ratio (HCR) was estimated as the ratio of concentrations for 10% surviving fraction (C_{10}) under aerobic and hypoxic conditions.

Determination of Bystander Effects in Multicellular Layer Cultures

Three-dimensional multicellular layer (MCL) cultures were grown from HCT116 cells (targets) or from 1:1 mixtures of targets and activators (HCT116-NTR^{puro}) as previously described (32). MCLs were exposed to nitro-CBI-5-[(dimethylamino)ethoxy]indole (DEI) for 5 h in stirred vessels under 5% CO_2/95% O_2 (to suppress hypoxia and thus endogenous metabolism by one-electron reductases), dissociated with trypsin, and plated with and without 3 μmol/L puromycin to determine clonogenic survival (32). The interpolated C_{10} values were calculated for targets alone (T), targets in cocultures (T_C), and activators in cocultures (A_C).

Determination of Metabolism of Nitro-CBI-DEI by Liquid Chromatography/Mass Spectrometry

Cell suspensions (2.5×10^6 or 5×10^6 cells/mL) were treated with nitro-CBI-DEI as for clonogenic assays. At various times, samples of 100 μL were withdrawn and precipitated with 400 μL acetonitrile (MeCN) containing 25 μmol/L bis (2-chloroethyl)-*N*-methyl-*N*-(4-methyl-2-nitrobenzyl)ammonium chloride (33) as internal standard (IS). Alternatively, cell suspensions were rapidly centrifuged, 100 μL of extracellular medium were extracted with 400 μL MeCN/IS, and the cell pellets were extracted with 100 μL MeCN/IS. Samples were stored at −80°C, thawed, and centrifuged

(12,000 × *g* for 5 min), and the supernatant was reduced to ~50 μL under vacuum. After addition of 100 μL of 0.45 mol/L ammonium formate buffer (pH 4.5)/MeCN (1:3, v/v), 100 μL of samples were analyzed by liquid chromatography/mass spectrometry (LC/MS) using an Agilent LC/MSD with a Zorbax 2.1 × 150 mm column (5 μm C8 packing) and a 45 mmol/L aqueous ammonium formate buffer (pH 4.5)/MeCN gradient. Detection was by diode array absorbance (nitro-CBI-DEI) and electrospray (positive mode) MS in scan mode or by selected ion monitoring at *m/z* 305 (IS) and 463 (amino-CBI-DEI), with a drying gas flow of 12 L/min, nebulizer pressure of 40 psig, drying gas temperature of 350°C, and capillary voltage of 4,000 V. Calibration curves (analyte/IS ratio versus analyte concentration) were constructed by spiking nitro-CBI-DEI or amino-CBI-DEI into each matrix (medium, cell pellets, and whole culture) and extracting with MeCN/IS in the same manner; for cell pellets, the analytes were added to the MeCN/IS solution.

Assay of the Amino-CBI-TMI Adenine Adduct in Cells

Single-cell suspensions (10^7 cells/mL) were prepared from RIF-1 tumors by enzymatic digestion using a cocktail of Pronase (0.5 mg/mL), collagenase (0.2 mg/mL), and DNase (0.2 mg/mL). Cells were exposed to amino-CBI-TMI or nitro-CBI-TMI as for clonogenic assays for 3 h. Cells were collected by centrifugation and pellets were lysed in 1 mL water containing 0.5 μmol/L of the previously reported (27) amino-CI-TMI adenine adduct as IS and heated to 70°C for 1 h to depurinate alkylated adenine bases. After cooling, samples were extracted with 1 mL dichloromethane in glass tubes and the organic layer was evaporated to dryness and reconstituted in 100 μL of DMSO and 30 μL was analyzed by LC/MS essentially as above by using an Alltima 3.2 × 150 mm column (C8 5 μm packing). Positive mode electrospray ionization was used for selective ion monitoring of nitro-CBI-TMI (*m/z* 496), amino-CBI-TMI (*m/z* 466), and the amino-CI-TMI and amino-CBI-TMI adenine adducts (*m/z* 515 and 565, respectively).

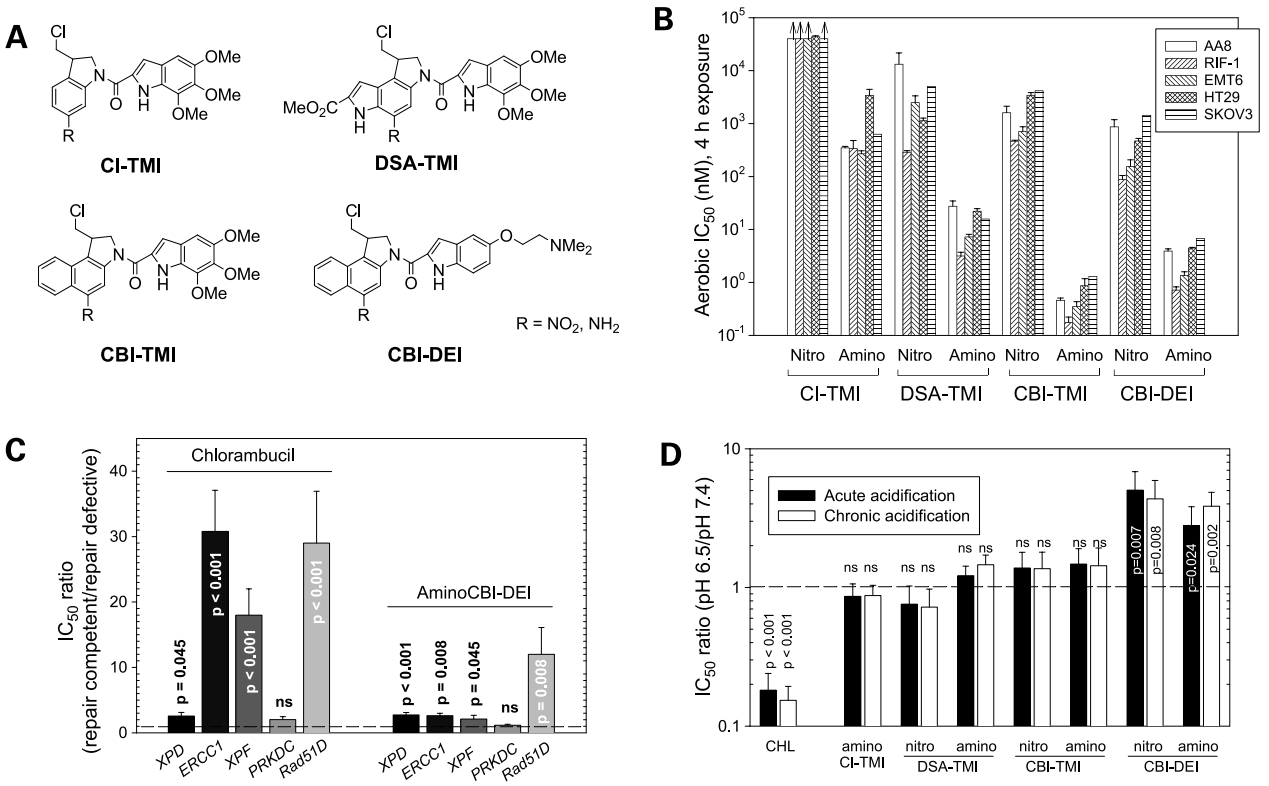

Figure 1. **A,** structures of compounds investigated. **B,** IC_{50} values following 4-h exposure of the indicated cell lines to compounds under aerobic conditions. Cell densities were evaluated by sulforhodamine B staining 4 to 5 d after drug washout. *Columns,* mean for three experiments; *bars,* SE. *Arrows* indicate values were above the solubility limit. **C,** IC_{50} ratios for repair-competent/repair-defective Chinese hamster cell line pairs exposed to amino-CBI-DEI or chlorambucil for 4 h under aerobic conditions. The cell line pairs were as follows: *XPD*, UV5 compared with AA8 (wild-type); *ERCC1*, UV4 compared with AA8; *XPF*, UV41 compared with its human XPF-complemented counterpart 41cER40.1; *PRKDC*, V3 compared with AA8; *Rad51D*, 51D1 compared with the hamster Rad51D-restored line 51D1.3. Values are ratios (mean ± root mean square SE) from 5 to 24 experiments. Significance of difference between cell line pairs (*t* test) are shown; ns indicates $P > 0.05$. Absolute IC_{50} values and sources of cell lines are reported in Supplementary Table S1. **D,** effect of acidification of cultures to pH 6.5 either acutely during the 4-h drug exposure or chronically for 18 h before and during drug exposure on IC_{50} for EMT6 cells. Values are ratios (mean ± root mean square SE) for two to five experiments. Significance of differences between pH 6.5 and 7.4 (*t* test) are shown. Absolute IC_{50} values are reported in Supplementary Table S2.

Determination of MTDs in Mice

Animal studies were approved by the University of Auckland Animal Ethics Committee (approval R256) and used specific pathogen-free animals bred and housed in the University of Auckland. Compound formulation and dosing is described in Supplementary Table S4. Initially, groups of three male C_3H/HeN mice were observed for 60 d, and the dose was adjusted using 1.33-fold (1/8th $\log_{10}$) dose increments as required to determine the MTD, which was defined as the highest dose causing no deaths or morbidity requiring euthanasia (e.g., >15% body weight loss) in a group of six mice.

Determination of Antitumor Activity in Mice

RIF-1 tumors were passaged alternately *in vitro* and *in vivo*, in female C_3H/HeN mice, using Twentyman's protocol (34). HCT8 and HT29 tumors were grown in female homozygous nude (CD1-Foxn1^{nu}) mice (Charles River Laboratories) by s.c. inoculation of 10^7 cells from tissue culture. Tumor growth was monitored thrice weekly with electronic calipers, and mice were randomized to treatment (specified in the figure legends) as tumors reached a mean diameter of 8 to 10 mm. Tumors were collected 18 h after treatment and dissociated enzymatically to determine clonogenic survivors per gram tumor as previously described (35). For tumor growth delay studies, RIF-1 tumors were grown in the gastrocnemius muscle and monitored by measurement of leg diameter. Mice were treated at a leg diameter of 9.5 to 10.5 mm, corresponding to a tumor weight of 0.4 to 0.6 g, and monitored until the end point (leg diameter of 13 mm, corresponding to 1.4 g tumors). Tumor growth delay was calculated as the difference in time to end point for control and treated tumors. Significance of treatment effects (growth delay or log cell kill for clonogens) was tested using ANOVA with Dunnett's multiple comparison test.

Results

Cytotoxic Potency of Amino- and Nitro-Chloromethylindolines

Three previously reported (26, 31, 36) synthetic variants of the alkylating subunit were evaluated (CI, DSA, and CBI) in combination with either a TMI or DEI sidechain; the structures are illustrated in Fig. 1A. Consistent with previous studies (26, 31, 36), the amino compounds (Fig. 1A, R = NH_2) potently inhibited cell proliferation in aerobic cultures (Fig. 1B). Potency increased in the order CI-TMI < DSA-TMI < CBI-DEI < CBI-TMI, with the latter providing subnanomolar IC_{50} values following 4-hour drug exposure. With the exception of the less potent amino-CI-TMI, the murine cell lines (RIF-1 and EMT6) were consistently more sensitive than the Chinese hamster (AA8) or human (HT29 and SKOV3) cell lines.

The cytotoxic potency of DNA minor groove alkylators may in part reflect the difficulty in repairing the resulting DNA lesions (37). We compared the sensitivity of Chinese hamster ovary cells with defects in specific DNA repair pathways to amino-CBI-DEI and the reference alkylator chlorambucil, which primarily cross-links guanine in the major groove. Cells with defects in the ERCC1-XPF endonuclease, which has a critical role in both nucleotide excision repair and homologous recombination repair (HRR; refs. 38, 39), or the Rad51 paralog Rad51D, which is essential for HRR (40), were markedly hypersensitive to chlorambucil (Fig. 1C; absolute IC_{50} values are shown in Supplementary Table S1) as recently reported (41). In contrast, the cytotoxicity of amino-CBI-DEI was less influenced by repair phenotype. Even in the Rad51D$^{-/-}$ cell line (51D1), which showed the greatest amino-CBI-DEI sensitivity relative to the corresponding isogenic wild-type (51D1.3), the differential was only one third of that for chlorambucil.

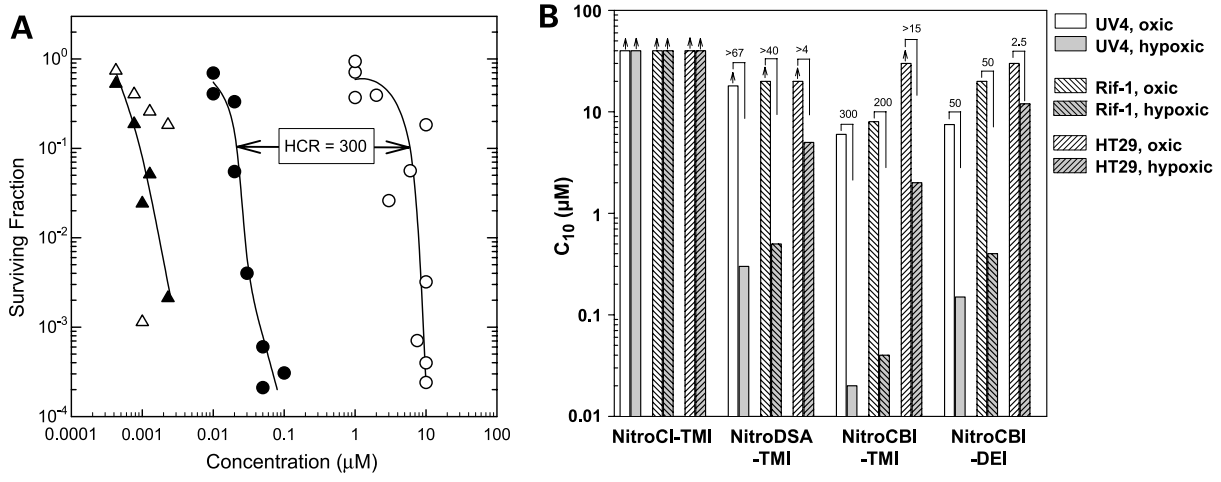

Figure 2. **A,** clonogenic cell killing by nitro-CBI-TMI (*circles*) and amino-CBI-TMI (*triangles*) in UV4 cell suspensions (10^6 cells/mL) following 4-h exposure under aerobic (*open symbols*) and hypoxic (*filled symbols*) conditions. Each point is a separate cell suspension; data are pooled from three experiments. The HCR was estimated as the ratio of C_{10} values (concentrations required for 10% survival) under aerobic versus hypoxic conditions. **B,** aerobic and hypoxic C_{10} values for the four nitro compounds against three cell lines exposed as stirred single-cell suspensions under the same conditions as in **A**. *Upward arrows,* C_{10} values above the solubility limit. HCR values are shown above the paired aerobic and hypoxic values.

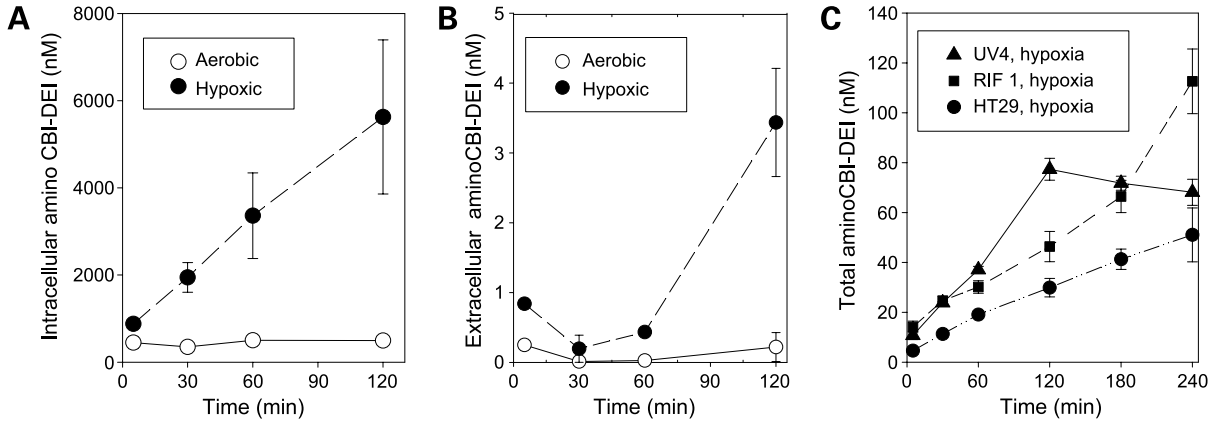

Figure 3. Hypoxia-selective metabolism of nitro-CBI-DEI (initial concentration, 10 μmol/L) by tumor cells. The amine metabolite (amino-CBI-DEI) was quantified by LC/MS. **A** and **B,** HT29 cell suspensions at 5×10^6 cells/mL. *Points,* mean for two cultures; *bars,* range. **A,** average intracellular concentration based on extraction of centrifuged cell pellets using the intracellular water content of HT29 cells (50). **B,** concentration in extracellular medium. **C,** comparison of total amino-CBI-DEI in three cell lines at 2.5×10^6/mL under hypoxia, determined by extracting whole cultures with acetonitrile. *Points,* mean for three cultures in the same experiment; *bars,* SE.

The nitro-chloromethylindolines were much less toxic than the corresponding amino compounds in all cases (Fig. 1B), with a pattern of sensitivity similar to that of the matching amino compound. Nitro/amino IC_{50} ratios were ~3,000 for CBI-TMI and in the range 90 to 480 for DSA-TMI and CBI-DEI, with the CI-TMI ratio indeterminate because of limited solubility of the nitro compound. These large nitro/amino differentials suggested the nitro compounds as candidate HAPs.

Because hypoxic cells often reside in an acidic microenvironment (42), we also tested whether lowering of extracellular pH from 7.4 to 6.5, either chronically for 18 hours before and during drug exposure or acutely during drug exposure, affected IC_{50} values for EMT6 cells (Fig. 1D; absolute IC_{50} values are shown in Supplementary Table S2). Chlorambucil, with a weakly acidic sidechain, showed a 5.5- and 6.5-fold increase in potency when pH was lowered to pH 6.5 acutely or chronically, respectively, as expected because of enhanced cellular uptake of weak acids at low extracellular pH (43). No significant effects of pH were observed for the neutral (TMI sidechain) compounds, but the two examples with a basic DEI sidechain showed a significant 2.8- to 5-fold reduction in potency at pH 6.5.

Hypoxia-Selective Cytotoxicity of Nitro-Chloromethylindolines *In vitro*

To test whether the nitro compounds are selectively toxic under hypoxic conditions, we exposed UV4, RIF-1, and HT29 cell lines as stirred single-cell suspensions under aerobic and hypoxic conditions and assessed cell killing using a clonogenic survival assay (Fig. 2). The illustrated dose response for nitro-CBI-TMI against UV4 cells (Fig. 2A) shows a large HCR of 300-fold. In contrast, amino-CBI-TMI showed no hypoxic selectivity (Fig. 2A). The ~20-fold lower potency of nitro-CBI-TMI than amino-CBI-TMI under hypoxia suggests that it is only partially metabolized to the amine under these conditions. Comparison of the four nitro compounds (Fig. 2B) showed a similarly large HCR for nitro-CBI-TMI in RIF-1 cells (~200-fold) but lower potency and selectivity against HT29. This same pattern was seen with nitro-DSA-TMI and nitro-CBI-DEI, although with lower HCR values (Fig. 2B).

Metabolism of Nitro-CBI-DEI to Amino-CBI-DEI under Hypoxia

To determine the mechanism of this hypoxia-selective cytotoxicity, we used stirred cell suspensions at high density (5×10^6/mL) to test whether UV4, RIF-1, and HT29 cells reduce nitro-CBI-DEI. Cellular uptake of the nitro compound (20 μmol/L) by HT29 cells was rapid (<5 minutes) and extensive, with intracellular concentrations ~5,000-fold higher than extracellular under both aerobic and hypoxic conditions (Supplementary Table S3). There was no significant change in total (intracellular plus extracellular) nitro-CBI-DEI over at least 4 hours in all three cell lines under either aerobic or hypoxic conditions (data not shown). However, amino-CBI-DEI was detected as a metabolite in hypoxic cultures of all cell lines by LC/MS, its structure being confirmed by comparison of retention time, absorbance spectrum, and mass spectrum with a synthetic standard (Supplementary Fig. S1). Quantitation of amino-CBI-DEI in HT29 suspensions during hypoxic incubation with 10 μmol/L nitro-CBI-DEI showed an approximately linear increase in the cells but no increase with time under aerobic conditions (Fig. 3A). By 2 hours, low concentrations of amino-CBI-DEI could also be detected in the extracellular medium of the hypoxic cultures (Fig. 3B). Summing the metabolite in both the intracellular and extracellular compartments (data not shown) gave an initial rate of metabolism of ~30 pmol/mL culture/h corresponding to 0.3% conversion of the prodrug per hour at this cell density (5×10^6 cells/mL), which is too slow a conversion to detect loss of the parent nitro compound. At half this cell density,

all three cell lines (UV4, RIF-1, and HT29) showed broadly similar rates of hypoxic metabolism of nitro-CBI-DEI to amino-CBI-DEI (Fig. 3C). Reduction of nitro-CBI-DEI to amino-CBI-DEI was also detected in hypoxic S9 preparations from HT29 cells and, at higher rates, from mouse liver (data not shown), whereas under aerobic conditions the sole metabolite identified (by MS^2 using ion trap MS) in mouse liver S9 was the tertiary amine *N*-oxide resulting from oxidation of the (dimethylamino)ethoxy sidechain (data not shown).

Selective Formation of the Adenine *N*3 Adduct in Hypoxic Cells

We showed reaction of amino-CBI-TMI with *N*3 of adenine in DNA by incubating the compound with calf thymus DNA at a 1:25 compound/base pair ratio followed by thermal depurination (see Supplementary Data for details). The major dichloromethane soluble product (89% yield) was the adenine *N*3 adduct **1** (Fig. 4A), which was fully characterized by nuclear magnetic resonance spectroscopy and MS. As shown in Fig. 4B, the same adenine adduct (**1**) was detected in RIF-1 cells following hypoxic incubation with nitro-CBI-TMI and heating to induce depurination, along with amino-CBI-TMI and an elimination product (loss of HCl) from nitro-CBI-TMI (**2**; Fig. 4A). The elimination product **2** was also seen in aerobic RIF-1 cells subject to the same heat treatment, but the reduction products (amino-CBI-TMI and adduct **1**) were not (Fig. 4B). Quantifying the adenine adduct by MS showed a concentration-dependent increase in the amino-CBI-TMI adduct (**1**) when RIF-1 cells were incubated under hypoxia with either amino- or nitro-CBI-TMI (Fig. 4C).

Bystander Effects from Metabolic Activation of Nitro-CBI-DEI in Three-Dimensional Cell Cultures

The observation that hypoxic cells exposed to nitro-CBI-DEI release amino-CBI-DEI into the extracellular medium (Fig. 3B) raised the question as to whether diffusion of this metabolite out of hypoxic zones might provide a bystander effect. To test this possibility in an experimentally accessible manner, we sought a model system in which cells capable of reductively activating nitro-CBI-DEI could be cocultured with (but distinguished from) a second population of nonmetabolizers. The *E. coli nfsB* nitroreductase (NTR) is well characterized as a broad-spectrum two-electron oxygen-insensitive nitroreductase and is known to activate nitro-CI-TMI (29). HCT116 cells that stably express NTR (HCT116-NTR^{puro} cell line) showed

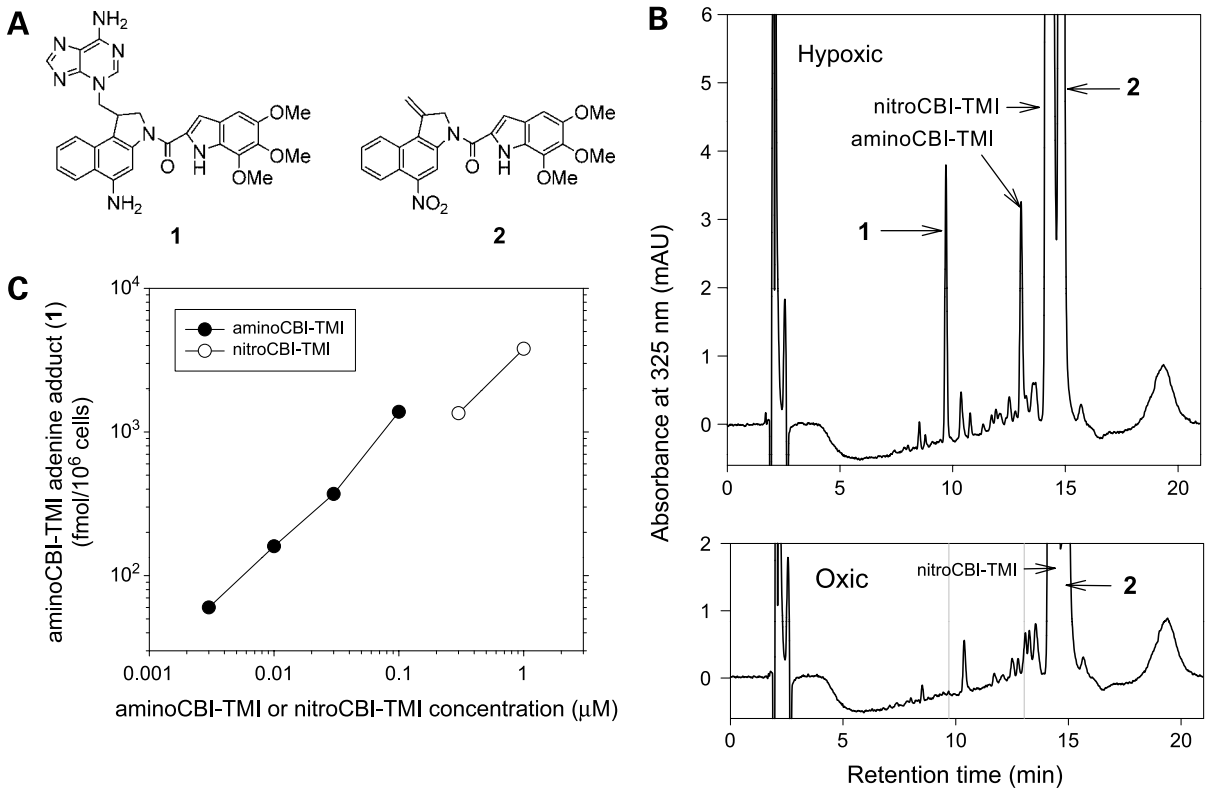

Figure 4. Alkylation of adenine *N*3 in DNA by amino-CBI-TMI and hypoxia-selective formation of the same adenine adduct from nitro-CBI-TMI in stirred suspensions of RIF-1 cells (10^7/mL). **A,** structures of amino-CBI-TMI *N*3 adenine adduct (**1**) and the HCl elimination product from nitro-CBI-TMI (**2**). **B,** chromatograms of dichloromethane extracts of RIF-1 cells incubated for 3 h under hypoxic (*top*) or oxic (*bottom*) conditions with 10 μmol/L nitro-CBI-TMI followed by heating to affect thermal depurination of alkylated bases. **C,** concentration of adenine adduct (**1**) in RIF-1 cells following incubation with amino-CBI-TMI (●) or nitro-CBI-TMI (○) under hypoxia for 3 h. Each point is a single cell culture.

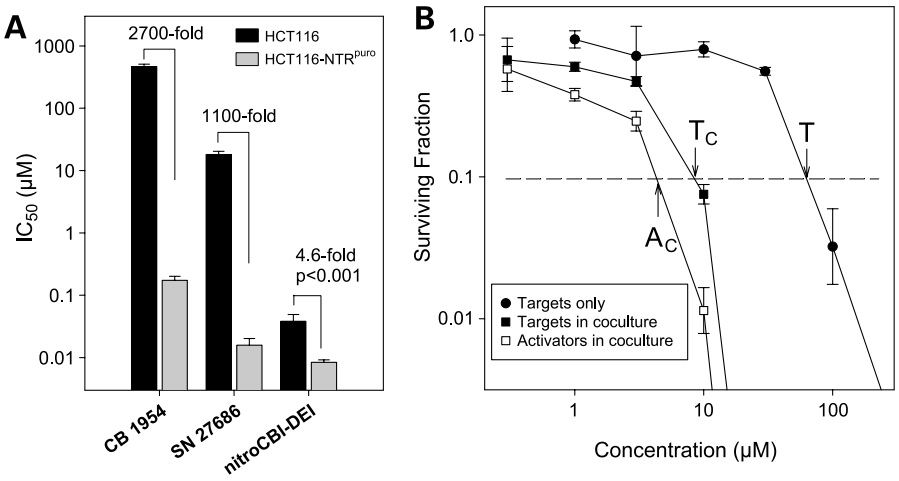

Figure 5. **A,** IC_{50} values after 18-h aerobic exposure of HCT116 cells, and cells stably transfected with the *E. coli nfsB* nitroreductase (HCT116-NTR^{puro}), to nitro-CBI-DEI and reference NTR substrates (dinitrobenzamides CB 1954 and SN 27686). **B,** clonogenic survival curves for HCT116 cells in MCLs exposed to nitro-CBI-DEI under aerobic conditions (95% O_2) for 5 h. MCLs were grown from parental NTR-negative HCT116 cells (targets) only or from 1:1 mixtures of targets and HCT116-NTR^{puro} cells (activators). *Points,* mean for three experiments, each with a single MCL at each nitro-CBI-DEI concentration; *bars,* SE. Concentrations for 1 log kill of targets alone (*T*), targets in cocultures (T_C), and activators in cocultures (A_C) were interpolated. The existence of a bystander effect is shown by the shift in the survival curves for targets when cocultured with activators.

the expected hypersensitivity to the dinitrobenzamides CB 1954 and SN 27686, which are known NTR prodrugs (Fig. 5A; ref. 32). Nitro-CBI-DEI showed a more modest (4.6-fold) but highly significant differential for the NTR-positive cells (Fig. 5A), suggesting this to be a poorer NTR substrate than the dinitrobenzamide prodrugs. However, NTR generated the same amino-CBI-DEI metabolite as endogenous reductases in hypoxic tumor cells (Supplementary Fig. S2), showing this to be a valid model for investigating bystander effects resulting from hypoxic metabolism of nitro-CBI-DEI.

We used the MCL three-dimensional cell culture model (18, 32) to test whether activation of nitro-CBI-DEI by HCT116-NTR^{puro} cells ("activators") is capable of killing NTR-null HCT116 cells ("targets") in these cocultures. MCLs were grown for 3 days from targets alone or 1:1 mixtures of activators and targets, the latter providing MCLs comprising 34.5 ± 2.5% (SE) activators as assessed by clonogenic assay of control MCLs in the presence and absence of puromycin. Determination of clonogenic cell killing (Fig. 5B) showed that cells in MCLs grown from targets alone were 12-fold less sensitive to nitro-CBI-DEI than NTR-positive activator cells in cocultures, as measured by the C_{10} ratio T/A_c. However, killing of targets was greatly increased in the cocultures, with target cells now only 2-fold less sensitive than activators themselves (T_c/A_c ratio). This shows an efficient bystander effect presumably resulting from reduction of nitro-CBI-DEI to its diffusible amino metabolite in a tissue-like three-dimensional cell culture system.

Toxicity of Nitro-CBI Prodrugs and Their Amine Effectors to Mice

Given the promising characteristics of the nitro-CBI compounds as HAPs in culture, we compared their toxicity to that of the corresponding amino metabolites following administration of single doses to mice. The relatively insoluble CBI-TMI compounds were formulated in 10% DMSO/40% polyethylene glycol/50% water (v/v/v) for i.p. administration. The MTD of amino-CBI-TMI (0.042 μmol/kg) was at least 500-fold lower than nitro-CBI-TMI, which was nontoxic at the highest dose that could be administered in solution (23.7 μmol/kg; Supplementary Table S4). Nitro-CBI-DEI could be formulated at higher concentrations, using 5% DMSO/20% polyethylene glycol/75% lactate buffer (pH 4.0; v/v/v), and gave MTD values of 31.6, 31.6, and 42.1 μmol/kg following i.p., i.v., and p.o. administration, respectively. Toxicity of amino-CBI-DEI varied markedly with route of administration, with MTD values of 0.0562, 0.562, and 7.5 μmol/kg for i.p., i.v., and p.o. dosing, respectively. Thus, the nitro-CBI-DEI was 560- to 5.6-fold less toxic than amino-CBI-DEI depending on the route of administration. Both amino compounds, and to a lesser extent nitro-CBI-DEI, at doses above the MTD caused late deaths (Supplementary Table S4). Deaths occurring >3 weeks after i.p. dosing were associated with i.p. organ adhesions, gastrointestinal tract obstruction, and histopathologic signs of chemical peritonitis at necropsy. The very low MTD of amino-CBI by the i.p. route presumably reflects this local toxicity, whereas its very high MTD by oral dosing suggests low oral bioavailability.

Activity of Nitro-CBI-DEI against Hypoxic Cells in Tumors

Given its superior formulation characteristics, evaluation of therapeutic activity focused on the basic analogue nitro-CBI-DEI. To test whether this kills hypoxic cells in tumors, we combined single i.p. doses of the drug with a dose of ionizing radiation sufficient to sterilize aerobic cells and assessed surviving clonogens 18 hours after treatment

(Fig. 6A–C). At its MTD, nitro-CBI-DEI by itself was inactive against RIF-1 tumors; however, it showed significant activity when dosed 5 minutes after irradiation (Fig. 6A). This activity was at least as great as the reference bioreductive drug tirapazamine at its MTD (the difference between nitro-CBI-DEI and TPZ was not statistically significant; Fig. 6A). Against HCT8 xenografts, nitro-CBI-DEI after irradiation again increased overall tumor cell killing, and the trend was similar in a third tumor model (HT29 xenografts), although in this case the effect of nitro-CBI-DEI after irradiation was not statistically significant.

Investigation of the time course of interaction with radiation against RIF-1 tumors (Fig. 6B) showed an apparent minimum in activity for drug 60 minutes before irradiation. In this experiment (with just three mice per group), the combination of nitro-CBI-DEI with radiation was not statistically different from radiation alone at any individual time point, but pooling the values for drug after (but not before) irradiation showed highly significant activity ($P = 0.005$). The dose response for nitro-CBI-DEI against RIF-1 tumors showed weak monotherapy activity, which was only statistically significant above the MTD (Fig. 6C). Dosing with nitro-CBI-DEI 5 minutes after irradiation showed greater activity than radiation alone, both at and above the MTD. At each dose level, the log cell kill additional to radiation alone was significantly ($P \leq 0.05$ by t test) greater than for drug only. Thus, nitro-CBI-DEI shows selective toxicity for hypoxic cells in RIF-1 tumors.

Given that the combination of TPZ 2 to 3 hours before cisplatin has been reported to be synergistic against RIF-1 tumors (44), we also evaluated nitro-CBI-DEI with cisplatin in this model using tumor growth delay as the end point (Fig. 6D). TPZ at MTD (270 μmol/kg) administered 2.5 hours before cisplatin provided a nonsignificant ($P = 0.08$) 3.3-day increase in growth delay over cisplatin alone. Nitro-CBI at its MTD (31.6 μmol/kg) gave modest but significant ($P = 0.016$) antitumor activity. Combination of nitro-CBI with cisplatin showed maximal activity when the compounds were coadministered, with addition of the nitro-CBI providing a highly significant ($P = 0.0017$) 5.6-day increase in tumor growth delay relative to cisplatin only.

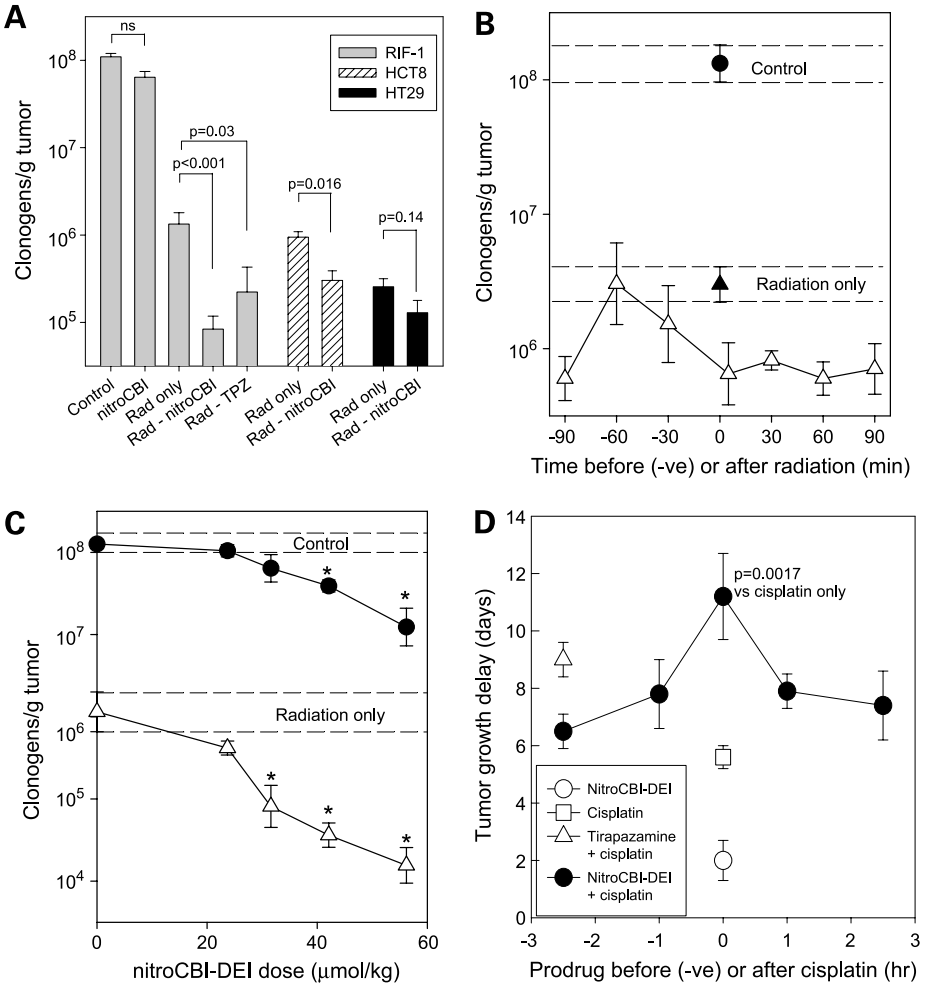

Figure 6. Antitumor activity of nitro-CBI-DEI in murine tumors (RIF-1) and human tumor xenografts (HCT8 and HT29). **A** to **C,** assayed by tumor excision and clonogenic assay 18 h after i.p. dosing with drug only or drug plus γ-irradiation. *Columns,* mean; *bars,* SE. **A,** nitro-CBI-DEI (31.6 μmol/kg) or tirapazamine (270 μmol/kg) 5 min after whole-body irradiation. RIF-1: radiation dose, 15 Gy; values pooled from three experiments each with three mice per group. HCT8: radiation dose, 15 Gy; four mice per group. HT29: radiation dose, 20 Gy; four mice per group. **B,** time course of interaction of nitro-CBI-DEI (31.6 μmol/kg) with radiation (15 Gy) against RIF-1 tumors (three mice per group). **C,** dose response for nitro-CBI-DEI alone (●) or 5 min after 15 Gy irradiation (Δ) against RIF-1 tumors (four mice per group). **D,** antitumor activity of nitro-CBI-DEI against RIF-1 tumors, in combination with cisplatin, as determined by tumor growth delay. Mice bearing s.c. RIF-1 tumors were treated with single i.p. doses of nitro-CBI-DEI alone (31.6 μmol/kg; ○), cisplatin alone (27 μmol/kg; □), and tirapazamine (270 μmol/kg) followed 2.5 h later by cisplatin (Δ) or nitro-CBI-DEI at various times before or after cisplatin (●). *Points,* mean for seven mice; *bars,* SE. All treatments showed significant activity ($P < 0.05$, relative to vehicle-only control). Of the combination groups, only coadministration with nitro-CBI provided significantly higher growth delay than cisplatin only ($P = 0.0017$).

Discussion

This study shows that highly potent amino-chloromethylindoline DNA minor groove alkylating agents can be generated by reductive metabolism of the corresponding nitro compounds in hypoxic tumor cells. The nitro-chloromethylindolines, and especially the chloromethylbenzindoline subclass (nitro-CBIs), therefore represent a novel HAP design with potential for targeting hypoxic cells in tumors.

The striking (approximately 90- to 3,000-fold) difference in cytotoxic potency between nitro- and amino-CBI compounds in aerobic cell cultures indicates that the nitro group powerfully suppresses DNA alkylation. This is consistent with the proposal that a strongly electron-withdrawing nitro group will inhibit spirocyclization to the active form of the alkylating subunit, whereas bioreduction to an electron-donating group can flip this electronic switch and promote DNA alkylation (29). In the small panel of cell lines investigated (Fig. 1B), there was a ~10-fold difference in aerobic sensitivity between the most sensitive (RIF-1) and resistant (HT29 and SKOV3) cell lines. The similar pattern for the nitro and amino compounds suggests that the differences in aerobic sensitivity to the nitro prodrugs are not a result of their aerobic activation in a subset of cell lines, unlike the situation with quinone or dinitrobenzamide HAPs, which are activated by variably expressed two-electron reductases (10, 12). Consistent with this, the lower hypoxic selectivity of the nitro prodrugs in HT29 relative to UV4 and RIF-1 reflects resistance under hypoxia rather than sensitivity under aerobic conditions [as would occur if, for example, the high activity of DT-diaphorase in HT29 cells (10) resulted in two-electron activation]. Thus, the HCR seems to be determined more by sensitivity to the amino metabolite than by differences in rates of reductive metabolism. The similarity in rates of hypoxic metabolism of nitro-CBI-DEI was confirmed by assay of the amino metabolite in these cell lines (Fig. 3C). Of note, the greater sensitivity of RIF-1 than HT29 cells to amino-CBI-DEI *in vitro* is paralleled by the greater sensitivity of RIF-1 than HT29 tumor xenografts (Fig. 6), although a larger series of cell lines needs to be investigated to determine what part the intrinsic sensitivity to the amino metabolites might play in determining antitumor activity.

The amino-CBIs represent attractive cytotoxic effectors for HAP design for reasons other than their high cytotoxic potency. One of their notable features is their insensitivity to DNA repair phenotype compared with the representative DNA interstrand cross-linking agent chlorambucil (Fig. 1C), suggesting that they represent "stealthy" lesions that are not readily recognized by repair pathways. Hypersensitivity of ERCC1 or XPF mutant cells to amino-CBI-DEI was even lower than reported for the achiral amino-CBI compound AS-I-145, for which mutation of either gene results in 7- to 8-fold hypersensitivity of Chinese hamster ovary cells (45). This insensitivity to ERCC1/XPF removes an important mechanism of resistance to cross-linking agents (46). HRR-defective Rad51D$^{-/-}$ cells show greater hypersensitivity, as expected, given that the cyclopropylindolines such as adozelesin are known to cause replication fork arrest (47) and that HRR has a key role in resolving such lesions (48), although dependence on HRR again seemed less than for chlorambucil.

Perhaps of even greater significance for HAP design, the amino-CBI-DEI metabolite is clearly able to elicit a bystander effect through diffusion from the cell in which it is formed. Not only is the amine observed as an extracellular metabolite in single cell cultures (Fig. 3B), but experiments using MCLs show the ability of this metabolite to kill surrounding cells in a tissue-like environment (Fig. 5B). These experiments exploited the finding that the *E. coli nfsB* nitroreductase (NTR) reduces nitro-CBI-DEI to the same amino metabolite as hypoxic reductases in tumor cells (Supplementary Fig. S2), and showed very efficient killing of NTR-negative bystander cells. This feature is considered to be a critically important requirement for maximally exploiting tumor hypoxia (5, 18) and particularly for avoiding the potential problem that many cells in tumors may not be sufficiently hypoxic to activate nitro or quinone HAPs but may still be hypoxic enough to be resistant to standard chemotherapy or radiotherapy (20, 49).

The nitro-CBI compounds evaluated in mice were markedly less toxic than the corresponding amines (Supplementary Table S4), suggesting that they do not undergo extensive systemic activation. We focused on the nitro-CBI-DEI prodrug for evaluation of antitumor activity because of its higher aqueous solubility, recognizing, however, that its basic sidechain has the potential to compromise potency against hypoxic cells if they are in acidic microenvironments. Nitro-CBI-DEI showed selectivity for hypoxic cells in RIF-1 tumors as indicated by greater activity in combination with radiation than for the prodrug alone. This differential (~2-fold; Fig. 6C) was much smaller than the hypoxic differential seen for RIF-1 cells in cell culture (50-fold; Fig. 2B). It is not yet clear whether this reflects the operation of a bystander effect (leading to hypoxia-dependent killing of oxic cells), inefficient killing of hypoxic cells because of poor extravascular diffusion of the prodrug, suppression of potency because of acidosis in hypoxic regions, or some other limitation. Although the antitumor activity of nitro-CBI-DEI against RIF-1 tumors is encouraging, significant activity (in combination with radiation and in combination with cisplatin) is only seen at or above the MTD (Fig. 6C and D). This inability to harness the full cytotoxic potential of the amino-CBI metabolite may reflect, in part, the relatively slow rates of cellular reduction of nitro-CBI-DEI by hypoxic cells *in vitro* (Fig. 3C). In summary, although systematic lead optimization is obviously required, nitro-CBI-DEI represents a promising proof of principle for a new class of HAPs.

Disclosure of Potential Conflicts of Interest

W.R. Wilson is a stockholder; W.R. Wilson and A.V. Patterson are consultants; and W.R. Wilson, F.B. Pruijn, S.P. Syddall, H.D.S. Liyanage, and M. Tercel have stock options in Proacta, Inc., which holds licenses related to the title compounds.

Acknowledgments

We thank Alan E. Lee for assistance with the animal studies, Sonia Alix for MS, Dr. Maruta Boyd for nuclear magnetic resonance spectroscopy, Dr. L. Jonathan Zwi (all University of Auckland) for evaluation of histopathology, and Dr. Larry H. Thompson (Brookhaven National Laboratory) who generously provided the repair-defective cell lines.

References

1. Lunt SJ, Chaudary N, Hill RP. The tumor microenvironment and metastatic disease. Clin Exp Metastasis 2009;26:19–34.

2. Brizel DM, Scully SP, Harrelson JM, et al. Tumor oxygenation predicts for the likelihood of distant metastases in human soft tissue sarcoma. Cancer Res 1996;56:941–3.

3. Fyles A, Milosevic M, Hedley D, et al. Tumor hypoxia has independent predictor impact only in patients with node-negative cervix cancer. J Clin Oncol 2002;20:680–7.

4. Nordsmark M, Bentzen SM, Rudat V, et al. Prognostic value of tumor oxygenation in 397 head and neck tumors after primary radiation therapy. An international multi-center study. Radiother Oncol 2005;77:18–24.

5. Brown JM, Wilson WR. Exploiting tumor hypoxia in cancer treatment. Nat Rev Cancer 2004;4:437–47.

6. Tatum JL, Kelloff GJ, Gillies RJ, et al. Hypoxia: importance in tumor biology, noninvasive measurement by imaging, and value of its measurement in the management of cancer therapy. Int J Radiat Biol 2006;82:699–757.

7. McKeown SR, Cowen RL, Williams KJ. Bioreductive drugs: from concept to clinic. Clin Oncol (R Coll Radiol) 2007;19:427–42.

8. Chen Y, Hu L. Design of anticancer prodrugs for reductive activation. Med Res Rev 2009;29:29–64.

9. Wardman P. Electron transfer and oxidative stress as key factors in the design of drugs selectively active in hypoxia. Curr Med Chem 2001;8:739–61.

10. Plumb JA, Workman P. Unusually marked hypoxic sensitization to indoloquinone EO9 and mitomycin C in a human colon-tumour cell line that lacks DT-diaphorase activity. Int J Cancer 1994;56:134–9.

11. Kim JY, Patterson AV, Stratford IJ, Hendry JH. The importance of DT-diaphorase and hypoxia in the cytotoxicity of RH1 in human breast and non-small cell lung cancer cell lines. Anticancer Drugs 2004;15:71–7.

12. Patterson AV, Guise CP, Abbattista M, et al. The bioreductive prodrug PR-104 is activated under aerobic conditions by human aldo-keto reductase 1C3 (prostaglandin F synthase). EJC Supplements 2008;6:473.

13. Hicks KO, Pruijn FB, Secomb TW, et al. Use of three-dimensional tissue cultures to model extravascular transport and predict *in vivo* activity of hypoxia-targeted anticancer drugs. J Natl Cancer Inst 2006;98:1118–28.

14. Phillips RM, Loadman PM, Cronin BP. Evaluation of a novel *in vitro* assay for assessing drug penetration into avascular regions of tumours. Br J Cancer 1998;77:2112–9.

15. Koch CJ. Unusual oxygen concentration dependence of toxicity of SR-4233, a hypoxic cell toxin. Cancer Res 1993;53:3992–7.

16. Lee AE, Wilson WR. Hypoxia-dependent retinal toxicity of bioreductive anticancer prodrugs in mice. Toxicol Appl Pharmacol 2000;163:50–9.

17. Parmar K, Mauch P, Vergilio J, Sackstein R, Down JD. Distribution of hematopoietic stem cells in the bone marrow according to regional hypoxia. Proc Natl Acad Sci U S A 2007;104:5431–6.

18. Wilson WR, Hicks KO, Pullen SM, et al. Bystander effects of bioreductive drugs: potential for exploiting pathological tumor hypoxia with dinitrobenzamide mustards. Radiat Res 2007;167:625–36.

19. Patterson AV, Ferry DM, Edmunds SJ, et al. Mechanism of action and preclinical antitumor activity of the novel hypoxia-activated DNA crosslinking agent PR-104. Clin Cancer Res 2007;13:3922–32.

20. Hicks KO, Myint H, Patterson AV, et al. Oxygen dependence and extravascular transport of hypoxia-activated prodrugs: comparison of the dinitrobenzamide mustard PR-104A and tirapazamine. Int J Radiat Oncol Biol Phys 2007;69:560–71.

21. Boger DL, Johnson DS. CC-1065 and the duocarmycins: understanding their biological function through mechanistic studies. Angew Chem Int Ed Engl 1996;35:1438–74.

22. Kobayashi E, Okamoto A, Asada M, et al. Characteristics of antitumor activity of KW-2189, a novel water-soluble derivative of duocarmycin, against murine and human tumors. Cancer Res 1994;54:2404–10.

23. Pavlidis N, Aamdal S, Awada A, et al. Carzelesin phase II study in advanced breast, ovarian, colorectal, gastric, head and neck cancer, non-Hodgkin's lymphoma and malignant melanoma: a study of the EORTC early clinical studies group (ECSG). Cancer Chemother Pharmacol 2000;46:167–71.

24. Tercel M, Denny WA, Wilson WR. Nitrogen and sulfur analogues of the seco-CI alkylating agent: synthesis and cytotoxicity. Bioorg Med Chem Lett 1996;6:2735–40.

25. Atwell GJ, Tercel M, Boyd M, Wilson WR, Denny WA. Synthesis and cytotoxicity of 5-amino-1-(chloromethyl)-3-[(5,6,7-trimethoxyindol-2-yl) carbonyl]-1,2-dihydro-3*H*-benz[e]indole (amino-seco-CBI-TMI) and related 5-alkylamino analogues: new DNA minor groove alkylating agents. J Org Chem 1998;63:9414–20.

26. Tercel M, Gieseg MA, Denny WA, Wilson WR. Synthesis and cytotoxicity of amino-seco-DSA: an amino analogue of the DNA alkylating agent duocarmycin SA. J Org Chem 1999;64:5946–53.

27. Tercel M, Gieseg MA, Milbank JB, et al. Cytotoxicity and DNA interaction of the enantiomers of 6-amino-3-(chloromethyl)-1-[(5,6,7-trimethoxyindol-2-yl)carbonyl]indo-line (amino-seco-CI-TMI). Chem Res Toxicol 1999;12:700–6.

28. Gieseg MA, Matejovic J, Denny WA. Comparison of the patterns of DNA alkylation by phenol and amino seco-CBI-TMI compounds: use of a PCR method for the facile preparation of single end-labelled double-stranded DNA. Anticancer Drug Des 1999;14:77–84.

29. Tercel M, Denny WA, Wilson WR. A novel nitro-substituted seco-CI—application as a reductively activated adept prodrug. Bioorg Med Chem Lett 1996;6:2741–4.

30. Tercel M, Denny WA. Synthesis of nitrogen and sulfur analogues of the seco-CI alkylating agent. J Chem Soc Perkin Trans 1998;Perkin Transactions 1:509–19.

31. Atwell GJ, Milbank JJ, Wilson WR, Hogg A, Denny WA. 5-Amino-1-(chloromethyl)-1,2-dihydro-3*H*-benz[*e*]indoles: relationships between structure and cytotoxicity for analogues bearing different DNA minor groove binding subunits. J Med Chem 1999;42:3400–11.

32. Singleton DC, Li D, Bai SY, et al. The nitroreductase prodrug SN 28343 enhances the potency of systemically administered armed oncolytic adenovirus ONYX-411 (NTR). Cancer Gene Ther 2007;14:953–67.

33. Tercel M, Wilson WR, Anderson RF, Denny WA. Hypoxia-selective antitumor agents. 12. Nitrobenzyl quaternary salts as bioreductive prodrugs of the alkylating agent mechlorethamine. J Med Chem 1996;39:1084–94.

34. Twentyman PR, Brown JM, Gray JW, et al. A new mouse tumor model system (RIF-1) for comparison of end-point studies. J Natl Cancer Inst 1980;64:595–604.

35. Singleton RS, Guise CP, Ferry DM, et al. DNA crosslinks in human tumor cells exposed to the prodrug PR-104A: relationships to hypoxia, bioreductive metabolism and cytotoxicity. Cancer Res 2009;69:3884–91.

36. Milbank JB, Tercel M, Atwell GJ, et al. Synthesis of 1-substituted 3-(chloromethyl)-6-aminoindoline (6-amino-seco-CI) DNA minor groove alkylating agents and structure-activity relationships for their cytotoxicity. J Med Chem 1999;42:649–58.

37. Brooks N, McHugh PJ, Lee M, Hartley JA. Alterations in the choice of DNA repair pathway with increasing sequence selective DNA alkylation in the minor groove. Chem Biol 2000;7:659–68.

38. De Silva IU, McHugh PJ, Clingen PH, Hartley JA. Defining the roles of nucleotide excision repair and recombination in the repair of DNA interstrand cross-links in mammalian cells. Mol Cell Biol 2000;20:7980–90.

39. Bergstralh DT, Sekelsky J. Interstrand crosslink repair: can XPF-ERCC1 be let off the hook? Trends Genet 2008;24:70–6.

40. Hinz JM, Tebbs RS, Wilson PF, et al. Repression of mutagenesis by Rad51D-mediated homologous recombination. Nucleic Acids Res 2006;34:1358–83.

41. Gu Y, Patterson AV, Atwell GJ, et al. Roles of DNA repair and reductase activity in the cytotoxicity of the hypoxia-activated dinitrobenzamide mustard PR-104A. Mol Cancer Ther 2009;8:1714–23.

42. Helmlinger G, Yuan F, Dellian M, Jain RK. Interstitial pH and pO2 gradients in solid tumors *in vivo*: high-resolution measurements reveal a lack of correlation. Nat Med 1997;3:177–82.

43. Denny WA, Wilson WR. Considerations for the design of nitrophenyl mustards as agents with selective toxicity for hypoxic tumor cells. J Med Chem 1986;29:879–87.

44. Dorie MJ, Brown JM. Tumor-specific, schedule-dependent interaction between tirapazamine (SR 4233) and cisplatin. Cancer Res 1993;53: 4633–6.

45. Kiakos K, Sato A, Asao T, et al. DNA sequence-selective adenine alkylation, mechanism of adduct repair, and *in vivo* antitumor activity of the novel achiral seco-amino-cyclopropylbenz[*e*]indolone analogue of duocarmycin AS-I-145. Mol Cancer Ther 2007;6:2708–18.

46. Felip E, Rosell R. Testing for excision repair cross-complementing 1 in patients with non-small-cell lung cancer for chemotherapy response. Expert Rev Mol Diagn 2007;7:261–8.

47. Liu JS, Kuo SR, Beerman TA, Melendy T. Induction of DNA damage responses by adozelesin is S phase-specific and dependent on active replication forks. Mol Cancer Ther 2003;2:41–7.

48. Thompson LH, Hinz JM. Cellular and molecular consequences of defective Fanconi anemia proteins in replication-coupled DNA repair: mechanistic insights. Mut Res-Fund Mol Mech Mutagen 2009;668:54–72.

49. Marshall RS, Rauth AM. Oxygen and exposure kinetics as factors influencing the cytotoxicity of porfiromycin, a mitomycin C analogue, in Chinese hamster ovary cells. Cancer Res 1988;48:5655–9.

50. Hicks KO, Pruijn FB, Sturman JR, Denny WA, Wilson WR. Multicellular resistance to tirapazamine is due to restricted extravascular transport: a pharmacokinetic/pharmacodynamic study in HT29 multicellular layer cultures. Cancer Res 2003;63:5970–7.